Russian Journal of Earth Sciences

Solving Inverse Magnetometry Problems Using Fuzzy Logic

S. M. Agayan[1], Sh. R. Bogoutdinov[*,1,2], and I. Y. Firsov[1]

[1] Geophysical Center RAS, Moscow, Russia
[2] Schmidt Institute of Physics of the Earth RAS, Moscow, Russia
* **Correspondence to:** Shamil Bogoutdinov, shm@gcras.ru.

Abstract: Integration interpretation of geophysical anomalies is a procedure for extracting geological and geophysical information about the object under study from observed physical fields. Interpretations are closely related to solutions of systems of linear algebraic equations (SLAE), therefore the possibility of the most complete and constructive description of all solutions of SLAE is of particular importance. It will allow you to take into account all additional information about the object and obtain the highest quality interpretation. The paper presents the authors' results on the constructive description of SLAE solutions and its application to the construction of gravimetric interpretations.

Keywords: system of linear algebraic equations; inverse magnetometry problem; constructive description of solutions; projection method.

Citation: Agayan, S. M., Sh. R. Bogoutdinov, and I. Y. Firsov (2024), Solving Inverse Magnetometry Problems Using Fuzzy Logic, *Russian Journal of Earth Sciences*, 24, ES4004, EDN: ZMRLJG, https://doi.org/10.2205/2024es000932

Introduction

Interpretation of geophysical anomalies is a process of extraction of information from observed physical field data, which contain a large amount of geological information in a hidden form. The main objective of data interpretation is to extract this information in order to solve a specific geological problem. Interpretation is not a strictly structured process, and to perform the task, the interpreter must be a skilled individual, and possess all the tools to extract the geological information from the geophysical fields. However, based on geophysical data alone, it is only possible to formally describe the distribution of physical properties, and there may be infinite amounts of examples of such distributions. Therefore, to perform a meaningful interpretation, all available a priori geological and geophysical information on the object under study is required. Interpretation is also mainly carried out within the framework of certain models, which is a set of simplifications and assumptions for this particular problem.

One of the principal methods for solving inverse problems of geophysics is the regularization method. The classic theory of regularization of systems of linear algebraic equations (SLAEs) was created in the works of Tikhonov, Ivanov, and Lavrentiev, as well as in multiple works of their follower in the 1960s–1980s [*Tikhonov and Arsenin*, 1979; *Turchin and Turovtseva*, 1973; *Zelenyi et al.*, 2018].

One of the objectives of the interpretation process is to determine the parameters of objects that create the studied anomaly field. Such problems are called "inverse problems", which refer to under determined problems of mathematical physics.

Existing methods for solving the inverse problems, such as the regularization technique, mostly search for a quasi-resolution, which may not be a solution to the source problem, but only an approximation to it.

In this study we consider an approach that allows us to describe a set of solutions that satisfy the problem and to search among these equivalent solutions for a model that best satisfies the available a priori information about the distribution of model properties.

A constructive description of the variety of solutions $\Phi(A, b)$ of a linear system $Ax = b$ in the finite-dimensional Euclidean space E allows us to consider a priori information about the properties of the desired solution x^f by searching for it on the variety $\Phi(A, b)$.

Research Article

Received: 17 November 2023
Accepted: 27 August 2024
Published: 15 October 2024

Technically, it looks like this: the expert point of view on the desired solution x^f is formalized by a non-negative functional F on $\Phi(A,b)$, and the solution x^f minimizes it. If there are several points of view on x^f and a system of functionals $\mathcal{F} = (F_1,\dots,F_k)$ is responsible for them, then the search for x^f is reduced to a multi-criteria choice $B(\Phi(A,b),\mathcal{F})$ relative to $\mathcal{F}$ on $\Phi(A,b)$.

The above is graphically conveyed by the diagram

$$Ax = b \to \Phi(A,b) \to \mathcal{F} \to B(\Phi(A,b),\mathcal{F}) \to x^f. \tag{1}$$

The first transition in (1) relates entirely to linear algebra and in this paper will be performed using the Gramm-Schmidt orthogonalization.

The second transition in (1) formalizes the a priori information about the sought solution x^f into a system of functionals $\mathcal{F}$ on the manifold $\Phi(A,b)$ and therefore requires a wide range of methods (fuzzy mathematics, machine learning, etc.).

We construct a formalization of three expert statements E_μ, E_S and their conjunctions $E_{\mu S} = E_\mu \wedge E_S$. Let us give their formulations:

- Statement E_μ: "the sought solution x^f is similar to the known vector μ".
- Statement E_S: let the coordinates in E be indexed by a known set I, so that any x of E can be considered as a function on I: $x : i \to x_i, i \in I$. Let us denote by S the partition $I = I_1 \vee \dots \vee I_k$ and consider a vector x to be S-homogeneous if it is constant on every I_k.
  E_S: "the desired solution x^f is S-homogeneous".
- Statement $E_{\mu S}$: "the sought solution x^f is similar to the vector μ and is homogeneous with respect to the partition S".

The third transition in (1) is a broad optimization of functionals from $\mathcal{F}$ on the manifold $\Phi(A,b)$, involving both classical continuous methods (gradient, penalty functions, etc.) and discrete ones (choice theory, neural networks, etc.).

In the present paper the optimization on $\Phi(A,b)$ is performed by analytical methods: the gradients of the functionals associated with statements E_μ, E_S, $E_{\mu S}$ will be explicitly found, and with their help the variants of the true solution x^f.

Examples illustrating theoretical constructions are mainly related to gravimetry and are of both artificial and natural origin.

Projection method

The initial space E is assumed to be n-dimensional Euclidean space with respect to the scalar product $(,)$.

In a linear system

$$Ax = b \equiv (a_i,x) = b_i;\ i = 1,\dots,m,\ x \in E, \tag{2}$$

A simultaneously means both the set of vectors a_i from E and the matrix $m \times n$ with vectors a_i as rows, $b = (b_i|_{i=1}^m)$.

The projection method, as applied to the system (2), consists in efficiently constructing the manifold of its solutions $\Phi(A,b)$. This problem was solved by the authors in [*Agayan et al.*, 2020] based on the systematic use of the orthoprojector $H(a)$ perpendicular to $a \in E$: $H(a) = 1 - \frac{aa^\top}{a^\top a}$ if $A \neq 0$, and $H(0) = 1$.

In the present paper, the Gramm-Schmidt orthogonalization will have a major role in the presentation of the projection method.

Homogeneous systems

For the homogeneous system $Ax = 0$ the solution space $\Phi(A,0)$ coincides exactly with the orthogonal addition in E to the subspace $L(A)$ generated by A: $\Phi(A,0) = L(A)^{\perp}$. Therefore to solve the system $Ax = b$ we have to construct an orthoprojector

$$H = H(A) : E \to L(A)^{\perp}.$$

Let us do this using the Gramm-Schmidt orthogonalization process: if $G = \{g_i|_{i=1}^{N}$, $N = \operatorname{rang} A\}$ its result for the set A: $G = \mathrm{GSh}(A)$, then

$$H(A)(x) = x - \sum_{i=1}^{N} \frac{(x, g_i)}{(g_i, g_i)} g_i \ \forall x \in E. \tag{3}$$

Inhomogeneous systems

The solution of the inhomogeneous system $Ax = b$ is the sum of the partial x^* and the homogeneous one, so $\Phi(A,b) = x^* + \Phi(A,0)$. In the search for the solution x^* we will use the equivalence given below and the realization of its right-hand side using GSh orthogonalization:

$$x \in \Phi(A,b) \equiv \begin{array}{l} x \text{ vector in } E, \text{ whose image } Ax \text{ is the} \\ \text{projection } b \text{ on the image } \operatorname{Im} A \text{ in } \mathbb{R}^m \end{array}.$$

The system $P = \{Ae_j|_{j=1}^{n}\}$ generates an image in $\operatorname{Im} A$ in $\mathbb{R}^m$. Let us apply the orthogonalization of GSh to P and obtain an orthogonal system $G = \mathrm{GSh}(P)$: $G = \{g_i|_{i=1}^{N}$, $N = \operatorname{rang} P\}$.

We need prototypes of y_i vectors g_i under mapping A: $Ay_i = g_i$. If we know vectors y_i, then

$$b = \sum_{i=1}^{N} \frac{(b, g_i)}{(g_i, g_i)} g_i = \sum_{i=1}^{N} \frac{(b, g_i)}{(g_i, g_i)} Ay_i = A\left(\sum_{i=1}^{N} \frac{(b, g_i)}{(g_i, g_i)} y_i \right).$$

Thus, the vector

$$x^* = \sum_{i=1}^{N} \frac{(b, g_i)}{(g_i, g_i)} y_i \tag{4}$$

will give us a partial solution to the system $Ax = b$.

We construct vectors g_i and y_i iteratively. We start with g_i: if $g_1, \ldots, g_{i-1}$, $i \geq 2$ are known, then according to GSh:

$$g_i = Ae_i - \sum_{k=1}^{i-1} \frac{(Ae_i, g_k)}{(g_k, g_k)} g_k. \tag{5}$$

Starting with $g_1 = Ae_1$.

If the vectors $y_1, \ldots, y_{i-1}$, $i \geq 2$ are known, then taking into account (5)

$$g_i = Ae_i - \sum_{k=1}^{i-1} \frac{(Ae_i, g_k)}{(g_k, g_k)} Ay_k = A\left(e_i - \sum_{k=1}^{i-1} \frac{(Ae_i, g_k)}{(g_k, g_k)} y_k \right).$$

Thus,

$$y_i = e_i - \sum_{k=1}^{i-1} \frac{(Ae_i, g_k)}{(g_k, g_k)} y_k. \tag{6}$$

Starting with $y_1 = e_1$.

To summarize: the effective parametrization of the variety of the solution $\Phi(A,b)$ of the linear system $Ax = b$ with the help of the GSh orthogonalization is the correspondence

$$x = x^* + Hs,\ s \in E, \tag{7}$$

where H and x^* are given by the formulas (3) and (4).

Example 1. *A system of linear equations is given $Ax = b$:*

$$A = \begin{pmatrix} 2 & -1 & 1 & 2 & 3 \\ 6 & -3 & 2 & 4 & 5 \\ 6 & -3 & 4 & 8 & 13 \\ 4 & -2 & 3 & 4 & 2 \end{pmatrix}; \quad b = \begin{pmatrix} 2 \\ 3 \\ 9 \\ 1 \end{pmatrix}. \tag{8}$$

After implementation Gramm-Schmidt orthogonalisations for the system $P = \{Ae_j|_{j=1}^n\}$, we obtain an orthogonal system $G = GSh(P)$: $G = \{g_i|_{i=1}^N, N = \operatorname{rang} P = 3\}$ (5)

$$\begin{array}{rcrrrr} g_1^\top & = & (\ 2.000, & 6.000, & 6.000, & 4.000); \\ g_2^\top & = & (-0.087, & -1.261, & 0.740, & 0.826); \\ g_3^\top & = & (\ 0.123, & -0.215, & 0.954, & -1.169). \end{array}$$

and the corresponding system Y: $Y = \{y_i|_{i=1}^N, N = \operatorname{rang} P = 3\}$ (6)

$$\begin{array}{rcrrrrr} y_1^\top & = & (\ 1.000, & 0.000, & 0.000, & 0.000, & 0.000); \\ y_2^\top & = & (-0.543, & 0.000, & 1.000, & 0.000, & 0.000); \\ y_3^\top & = & (-0.231, & 0.000, & -1.415, & 1.000, & 0.000). \end{array}$$

By substituting the calculated g_i, y_i, $i = 1,2,3$ into (4), we obtain a partial solution to our system

$$x^* = (-0.5,\ 0.0,\ -3.0,\ 3.0,\ 0.0).$$

The discrepancy in the solution obtained is $\|Ax - b\| = 8.189e^{-15}$.

Statement E_μ

The variety $\Phi(A,b)$ serves as the domain of determining an arbitrary statement about the true solution x^f. We will begin with the most basic of these, namely, the statement E_μ about the similarity of x^f to the known vector μ of E. Two interpretations will be given and analyzed.

First Interpretation

In this case, the similarity of x^f and μ is understood metrically as proximity in E: "x^f is the closest point to μ on the variety of solutions $\Phi(A,b)$".

If $x^* + Hs$ parameterizes $\Phi(A,b)$ (7), then the solution $\tilde{x}^f = x^* + HS^f$, which is a variant of the true solution x^f based on this interpretation of statement E_μ, is reduced to unconditional minimization by s on E the first version of the F_μ function:

$$F_\mu(s) = \left\|x^* + Hs - \mu\right\|^2; \quad \operatorname{grad} F_\mu(s) = H^\top Hs - H^\top(\mu - x^*), \tag{9}$$

which leads to a linear system of equations on the sought parameter s^f:

$$H^\top Hs^f = H^\top(\mu - x^*), \tag{10}$$

which can be solved by the projection method.

Example 2. *For the system* (8) *we will look for a solution close to the known vector* μ. *As* μ *a zero vector is taken, so in this case the problem is reduced to finding the minimum by norm solution* x^f.

To solve the problem, just construct the projector H [*Agayan et al.*, 2020] *and, assuming* $A = H^\top H$, $b = -H^\top x^*$, *find* s^f (10). *Using the* (3)–(10) *approach described above, we get* s^f *and* x^f:

$$\begin{aligned} s^f &= (48.500, \quad -24.000, \quad 0.000, \quad 0.000, \quad 0.000); \\ x^f &= (-0.108, \quad 0.054, \quad -0.084, \quad 0.084, \quad 0.729). \end{aligned}$$

The uncertainty of the resulting solution $\left\|Ax^f - b\right\| = 6.286e^{-14}$. *The norm of* $\left\|x^f\right\| = 0.74849$, *while the norm of* x^* *from the example 1 is* 4.27200.

Second Interpretation

This version of the similarity of x^f and μ is more invariant with respect to μ and in a sense semicorrelated: "x^f is the closest point on $\Phi(A, b)$ to the line $L(\mu)$ generated by vector μ".

In this case, the search for $\tilde{x}^f = x^* + Hs$ (a variant of x^f based on statement E_μ) is reduced to absolute minimization by s and t on the product $E \times \mathbb{R}$ of the second version of the F_μ functional:

$$F_\mu(s) = \left\|x^* + Hs - \mu t\right\|^2.$$

The desired pair of parameters (s^f, t^f) is obtained as a solution to a linear system

$$\begin{pmatrix} H^\top \mu & -H^\top \mu \\ -\mu^\top H & ||\mu||^2 \end{pmatrix} \begin{pmatrix} s^f \\ t^f \end{pmatrix} = \begin{pmatrix} -H^\top x^* \\ (x^*, \mu) \end{pmatrix}$$

and $x^f = x^* + Hs^f$.

Example 3. *This example is related with the inverse problem of gravimetry on a two-dimensional model with a given density grid* ρ (*Figure 1*).

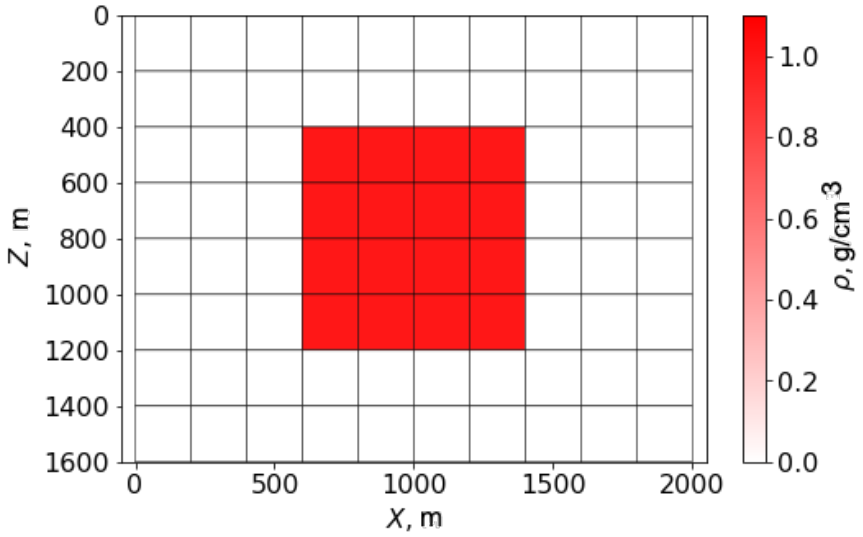

Figure 1. Density grid.

In this case x_j – the unknown density in jth rectangular cell with vertices σ_ν^j, $\nu = 1,2,3,4$; b_i – the value of the observed field at point s_i on the surface; a_{ij} – the conversion factor for the density j-th cell in the attraction at ith observation point. We have:

$$b_i = \sum_j a_{ij} x_j,$$

$$a_{ij} = Re(G(s_i, \sigma^j)).$$

The complex gravitational potential $G(s,\sigma)$ is calculated using the formula [Bulychev et al., 2010]:

$$G(s,\sigma) = G\delta \sum_{\nu=1}^{N} (\alpha_\nu s + \beta_\nu - \overline{s}) \ln \frac{\sigma_{\nu+1} - s}{\sigma_\nu - s},$$

$$\alpha_\nu(\sigma) = \frac{\overline{\sigma}_{\nu+1} - \overline{\sigma}_\nu}{\sigma_{\nu+1} - \sigma_\nu},$$

$$\beta_\nu(\sigma) = \overline{\sigma}_\nu - \alpha_\nu \sigma_\nu,$$

where G is the universal gravitational constant, δ is the density of the cell (in this case taken as unit), σ_ν is the complex coordinate of the $\nu - th$ vertex of the quadrangle, $\overline{s}$ and $\overline{\sigma}$ are complex conjugate quantities.

Figure 2 shows a given density distribution ρ and a priori information μ, which is equal to a slightly noisy half of the original model density.

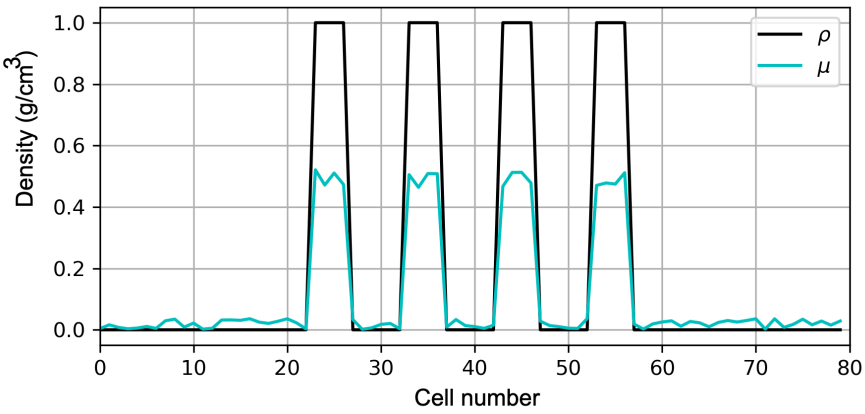

Figure 2. Source model density and a priori information.

Figure 3 shows the density distributions x^f and x^T found, respectively, using the projection method (10) and the Tikhonov regularisation method [Tikhonov and Arsenin, 1979] with $\alpha = 0.1$. It can be seen that while the Tikhonov regularisation method adds uninformative background values to the a priori model, the method under study uses a priori information in order to find a similar solution on the variety of solutions. This way, the main information is concentrated where the interpreter wants it to be.

1. *Solution evaluation by projection method (scheme (10)):*

$$\left\| x^f - \rho \right\| = 0.4382, \qquad \left\| Ax^f - b \right\| = 5.305e^{-7}.$$

2. *Evaluation of the solution by the Tikhonov regularization method ($\alpha = 0.001$):*

$$\left\| x^T - \rho \right\| = 1.7667, \qquad \left\| Ax^T - b \right\| = 1.062e^{-2}.$$

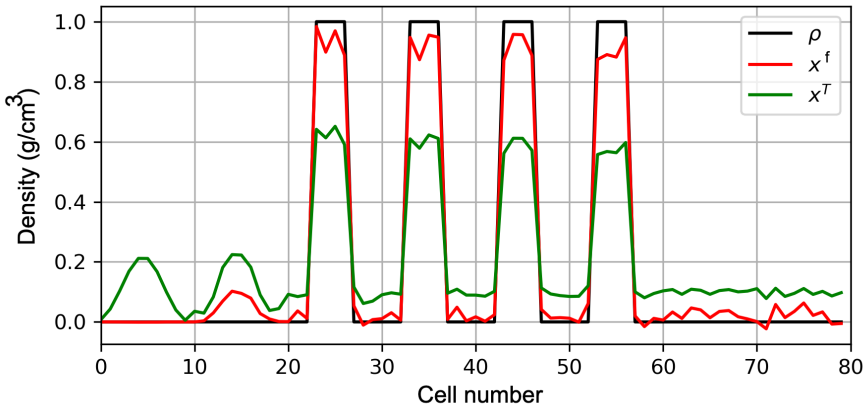

Figure 3. Comparison of solutions with the initial model.

Statement E_S

Let the coordinates in the space $E = \mathbb{R}^N(x)$ be indexed by the set I ($N = |I|$), so that any vector $x \in E$ can be considered a function on I: $x: i \to x_i, i \in I$.

Let us denote by S the disjunctive partition $I = I_1 \vee \cdots \vee I_K$, $S = \{I_k|_{k=1}^K\}$ and consider the vector x S-homogeneous if it is constant on each block $I_k, k = 1,\ldots,K$. Let us formulate a statement E_S:

E_S: "the true solution x^f of the system $Ax = b$ S-homogeneous".

The attention to E_S is not accidental, since homogeneity –a fundamental property of nature (we can just look at geology).

Formalization E_S

Any vector $x \in E$ is naturally associated with a S-homogeneous vector, which we call S-averaging x and denote by $M_S x$:

$$(M_S x)_i = \frac{\sum_{j \in I_k} x_j}{|I_k|}, \text{ if } i \in I_k. \tag{11}$$

The correspondence $x \to M_S x$ – projector in E, the quadratic deviation $F_S(x)$ from which quantitatively characterizes the S-homogeneity of x and thus formalizes the statement E_S

$$F_S(x) = \|x - M_S x\|^2. \tag{12}$$

Let us represent $F_S(x)$ through intra-block homogeneity uncertainties. To do this, denote by pr^k: $E \to \mathbb{R}^{|I_K|}$ the mapping of constraint x to block I_k: $x \to x^k = x|_{I_k}$, and by $F_k(x) = \left\|x^k - \overline{x^k}\right\|^2$ the deviation x^k from its mean $\overline{x^k}$.

This deviation can be understood as an inverse quantitative characteristic of the homogeneity of the vector $x^k \in \mathbb{R}^{|I_k|}$ with respect to the trivial partition of the block I_k consisting only of itself. Therefore

$$\left\|x^k - \overline{x^k}\right\|^2 = F_{I_k}(x^k) \text{ and } F_k(x) = F_{I_k}(\mathrm{pr}^k x). \tag{13}$$

From the very definition (12) of the function $F_S(x)$ follows the equality

$$F_S(x) = \sum_{k=1}^K F_k(x). \tag{14}$$

For any i of block I, the equality $|x_i - M_S x|^2 = |x_i - \overline{x^k}|^2$ is true.

Gradient E_S

The calculation of the gradient $\operatorname{grad} F_k(x)$ is much related to the calculation of the gradient $\operatorname{grad} F_{I_k}(x^k)$. Without loss of generality, we do this below for the function $F_I(x)$ in E. The gradients $\operatorname{grad} F_{I_k}(x^k)$ must then be assembled together using the projectors $\mathrm{pr}^k x$ to obtain $\operatorname{grad} F_S(x)$ (14). Let us do this first for the so-called S partition consistent with I, and then reduce the general case of S to a consistent one.

Each block I_k of partition S has within it an ordering $I_k = \{i_1^k < \cdots < i_{|I_k|}^k\}$, induced by the outer ordering on I: $I = \{i_1 < \cdots < i_N\}$.

Thus, any index i has two coordinates $i = i_j^k$ associated with the partition S besides its main number m in I: $i = i_m$, $m = m(i)$:

$k = k(i, S)$ – the number of the block I_k of partition S, which includes index i;
$j = j(i, S)$ – internal index number i directly in block I_k.

Call a partition S consistent with I if

$$m(i) = \sum_{k<k(i,S)} |I_k| + j(k, S), \ \forall i \in I. \tag{15}$$

Informally, this means that S is a partition of I into consecutive segments $I_1 = \{i_1, \ldots, i_{|I_1|}\}$, $I_2 = \{i_{|I_1|+1}, \ldots, i_{|I_1|+|I_2|}\}$ and so on.

Let us find $\operatorname{grad} F_S(x)$ for such S and start, as mentioned above, by calculating the gradients $\operatorname{grad} F_{I_k}(x^k)$ for all $k = 1, \ldots, K$ on the example $\operatorname{grad} F_I(x)$.

So, $x = (x_1, \ldots, x_N)$, $N = |I|$

$$F_I(x) = \sum_{i=1}^{N} \left(x_i - \frac{\sum_{j=1}^{N} x_j}{N} \right)^2 = \sum_{i=1}^{N} \frac{\left((N-1)x_i - \sum_{j \neq i} x_j\right)^2}{N^2}.$$

By selecting the coordinate x_1, calculate the derivative $\frac{\partial F_I}{\partial x_1}$

$$F_I(x) = \frac{\left((N-1)x_1 - x_2 - \cdots - x_N\right)^2}{N^2} + \frac{\left(-x_1 + (N-1)x_2 - \cdots - x_N\right)^2}{N^2} + \\ + \cdots + \frac{\left(-x_1 - x_2 - \cdots + (N-1)x_N\right)^2}{N^2}$$

Taking the derivative, we get

$$\frac{\partial F_I(x)}{\partial x_1} = \frac{(N-1)}{N^2}\left((N-1)x_1 - x_2 - \cdots - x_N\right) - \frac{1}{N^2}\left(-x_1 + (N-1)x_2 - \cdots - x_N\right) - \\ - \cdots - \frac{1}{N^2}\left(-x_1 - x_2 - \cdots + (N-1)x_N\right)$$

After transformations we get the following equality

$$\frac{\partial F_I(x)}{\partial x_1} = x_1 - \frac{1}{N}\sum_{i=1}^{N} x_i.$$

Similarly for x_k, $k > 1$

$$\frac{\partial F_I(x)}{\partial x_k} = x_k - \frac{1}{N}\sum_{i=1}^{N} x_i.$$

So that

$$\operatorname{grad} F_I(x) = x - \frac{\operatorname{tr} x}{N}\vec{1} = \left(1_N - \frac{1}{N}E_N\right)(x),$$

where $\vec{1}$ is a vector with unit coordinates from E, 1_N (E_N) — identity matrix (constant matrix with unit elements) of order N.

Recalling that $N = |I|$, let

$$G_I = 1_{|I|} - \frac{1}{|I|}E_{|I|},$$

and conclude: for $k = 1,\dots,K$

$$\operatorname{grad} F_{I_k}(x^k) = G_{I_k}(x^k),$$

where

$$G_{I_k} = 1_{|I_k|} - \frac{1}{|I_k|}E_{|I_k|}.$$

Due to the consistency of the partition S with I, the union of the gradients $\operatorname{grad} F_{I_k}(x^k)$ is given by the product of the block matrix $G_S = \{G_{I_k}|_{k=1}^K\}$ and vector x in the representation $x = (x^k|_{k=1}^K)$:

$$\operatorname{grad} F_S(x) = G_S(x) = \begin{Vmatrix} G_{I_1} & & 0 \\ & \ddots & \\ 0 & & G_{I_K} \end{Vmatrix} \cdot \begin{Vmatrix} x^1 \\ \vdots \\ x^K \end{Vmatrix}.$$

If the partition S is not consistent with I in coordinates x, then, keeping the same notation S, the transition in space E from coordinates x to new coordinates y:

$$x_i = y_{\sum_{k<k(i,S)}|I_k| + j(i,S)},$$

we obtain the consistency of the partition S with the set of indices I in coordinates y (15).

Using the invariance of S-homogeneity from coordinates, let us calculate the S-homogeneity of any vector x of E in its y-coordinates

$$F_S(x) = F_S(y(x)).$$

Hence, taking into account the rule of differentiation of the superposition we have the gradient in the general case

$$\operatorname{grad} F_S(x) = S^\top G_S S x.$$

The last step in formalizing the statement E_S – the superposition of the functional $F_S(x)$ with the parameterization $x = x^* + Hs$, which we denote by $F_S(s)$ and give its gradient

$$\operatorname{grad} F_S(s) = H^\top S^\top G_S S(x^* + Hs). \tag{16}$$

To summarize: the search for the true solution $x^f = x^* + Hs : a$ based on S-homogeneity reduces to the solution of the linear system

$$H^\top S^\top G_S S H s^f = -H^\top S^\top G_S S x^*. \tag{17}$$

In its pure form, statement E_S tells only about the S-homogeneity of the true solution x^f, which is highly ambiguous and therefore ineffective.

To reduce the ambiguity of statement E_S, we need to connect it to some other statement about x^f. We do this below by connecting the statement E_S with the statement E_μ in the first treatment.

Statement $E_{\mu S}$

The conjunction $E_{\mu S}$ = {desired solution x^f of the system $Ax = b$ is similar to the vector μ and S-homogeneous} will be realized by the α-linear connection $F_\alpha(s)$ of functionals $F_S(s)$ (16) and $F_\mu(s)$ (9); $\alpha \in [0,1]$:

$$F_\alpha(s) = F_{\mu S}^\alpha(s) = \alpha F_S(s) + (1-\alpha)F_\mu(s) \tag{18}$$

Then

$$\operatorname{grad} F_\alpha(s) = \alpha H^\top S^\top G_S S(x^* + Hs) + (1-\alpha)(H^\top Hs - H^\top(\mu - x^*))$$

and therefore finding the true solution $x^f = x^* + Hs^f$ based on the statement $E_{\mu S}$ is reduced to solving a linear system

$$(\alpha(SH)^\top G_S SH + (1-\alpha)H^\top H)s^f = -\alpha(SH)^\top G_S Sx^* + (1-\alpha)H^\top(\mu - x^*). \tag{19}$$

The last part of this article is devoted to examples of inference (19) based on judgement $E_{\mu S}$.

Synthetic point example of finding a solution using the $F_{s\mu}$ functional

Let us consider the obtained results of solving the inverse problem from the point of view of closeness to the true density distribution.

Let us construct a two-dimensional synthetic model with 32×32 points horizontally and vertically. The distance between the points is 129 m horizontally and 32 m vertically. As points we take spheres with radius $R = 10$ m approximated by points. The observed effect is calculated by the formula (20).

$$V_z = G\frac{4}{3}\pi R^3 \sigma \frac{\zeta - z}{((\xi - x)^2 + (\gamma - y)^2 + (\zeta - z)^2)^{3/2}}, \tag{20}$$

where x, y, z are coordinates of the observation point, ξ, γ, ζ are coordinates of the center of the sphere, G is the gravitational constant, R is the sphere radius, σ is the sphere density.

The system $Ax = b$ describes the gravitational effect of the density environment. The system of linear equations can be written as follows:

$$\begin{aligned} &a_{11}x_1 + a_{12}x_2 + \cdots + a_{11}x_n = b_1 \\ &a_{21}x_1 + a_{22}x_2 + \cdots + a_{21}x_n = b_2 \\ &\cdots \\ &a_{m1}x_1 + a_{m2}x_2 + \cdots + a_{m1}x_n = b_m, \end{aligned} \tag{21}$$

where x_i are the unknown densities, a_{ji} is the effect of the i-th sphere with unit radius at observation point j, b_j is the value of the observed field at point j.

The structure of the model is the disjunctive union into 2×2 blocks (Figure 4). The densities of points on the grid vary from 1 to 4, but they are the same in blocks 2×2 (Figure 5a).

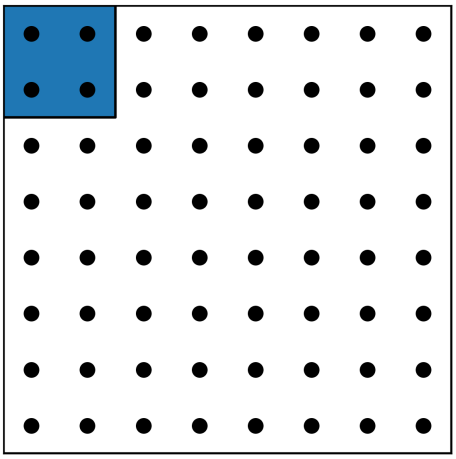

Figure 4. Explanation of combining grid points into block structures.

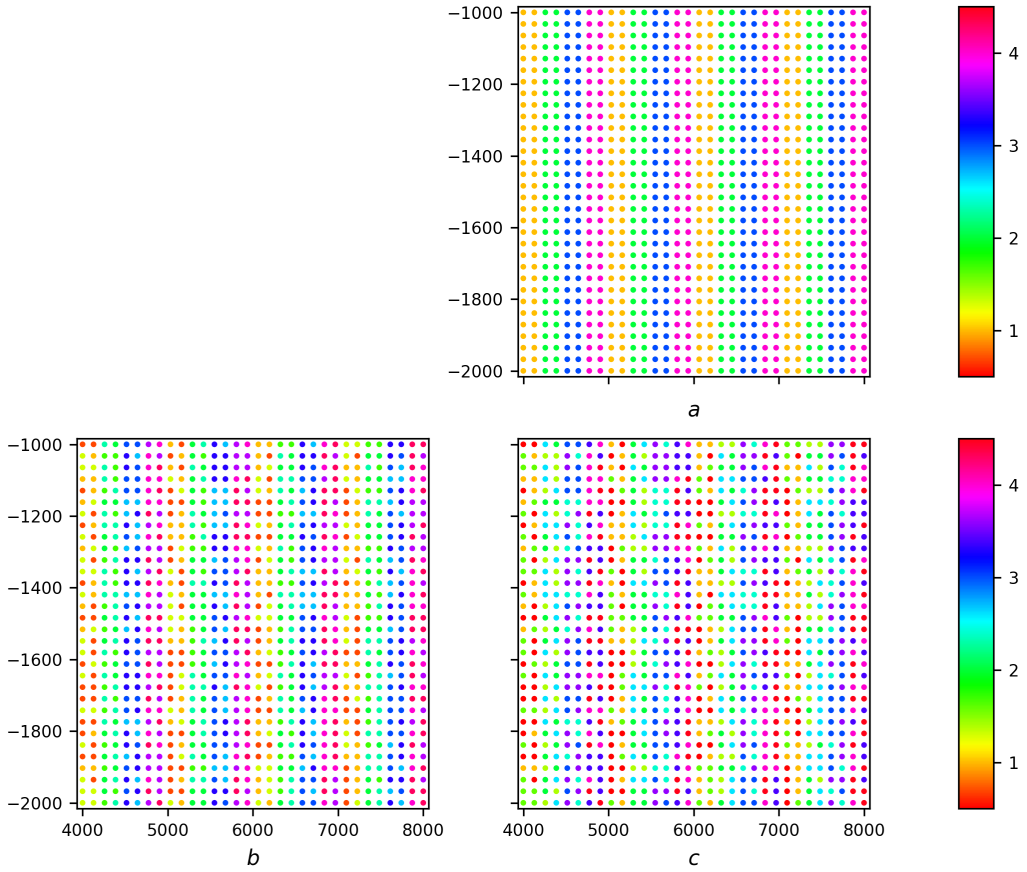

Figure 5. *a* – initial density distribution (ρ);
b – μ_1=ρ+random noise 10%; *c* – μ_2=ρ+random noise 20%.

The number of observation points is 51 in the range from 0 to 12,000 m. Figure 6 shows the response on the surface of the initial density distribution (Figure 5a).

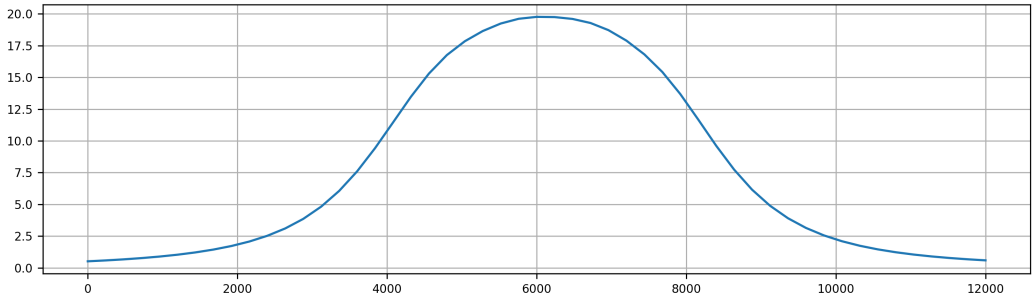

Figure 6. Response on the surface from the original density distribution.

To test the performance of the $F_{s\mu}$ functional, we introduce two vectors μ_1 (Figure 5b) and μ_2 (Figure 5c), which are equal to the original point density (Figure 5a) with the addition of random noise of maximum amplitude 10 and 20 percent, respectively, of the scatter of the original density, and consider its results on the 2×2 block system at α = 0.0, 0.1, 0.5, 0.99.

Figure 7 shows the results of finding solutions for the a priori density distribution μ_1 (Figure 5b). The Table 1 summarizes the quality criteria for the obtained solutions.

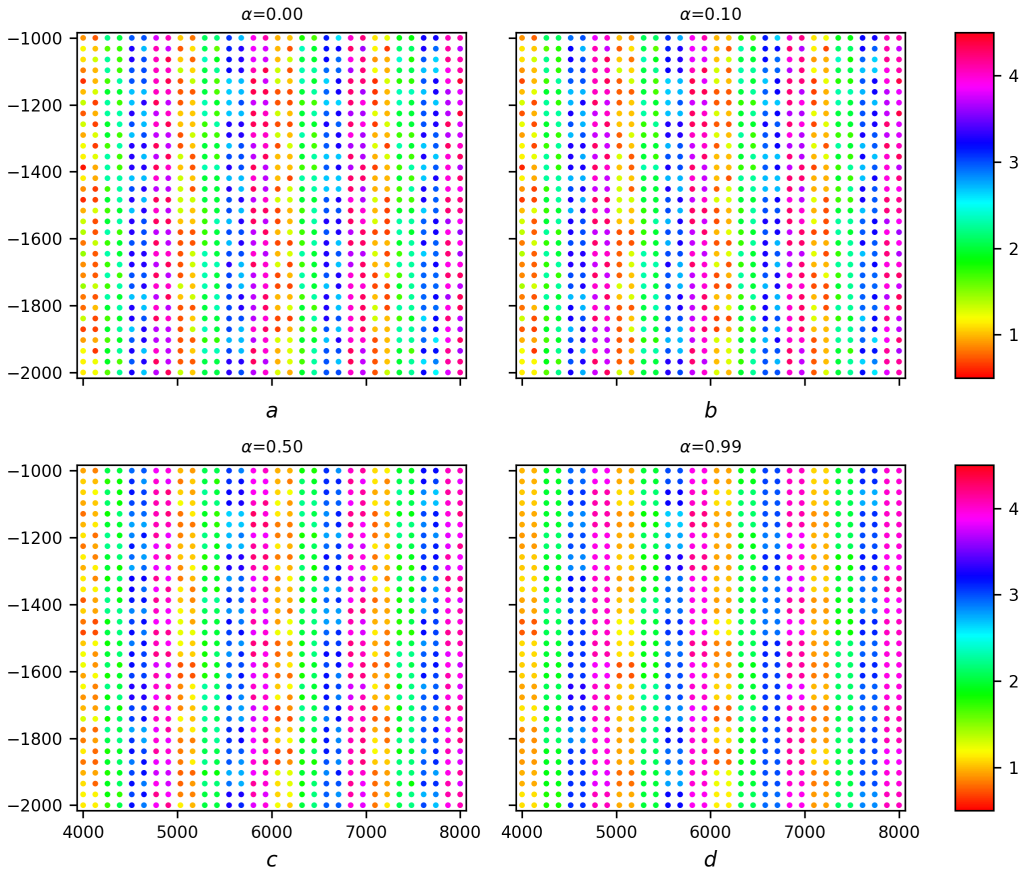

Figure 7. Finding a solution using the $F_{s\mu_1}$ functional on blocks 2×2: a – $\alpha = 0.0$, b – $\alpha = 0.1$, c – $\alpha = 0.5$, d – $\alpha = 0.99$.

Table 1. Quality criteria of obtained solutions for a priori distribution of densities μ_1

	Homogeneity	Closeness to ρ	Final criterion
$\alpha = 0.00$	—	7.69714	7.69714
$\alpha = 0.10$	6.18796	7.07885	6.98976
$\alpha = 0.50$	3.44360	4.85407	4.14883
$\alpha = 0.99$	0.07234	3.38303	0.10545

The Figure 8 shows the results of finding solutions for the a priori density distribution μ_2 (Figure 5c). The Table 2 summarizes the quality criteria for the obtained solutions.

Analysis of the Table 1 and Table 2 shows that as the parameter α increases, the homogeneity criterion and the criterion of closeness to ρ decreases. The final quality criterion at $\alpha = 0.99$ is much better, since the method, gives more weight to information about the uniform distribution of densities within blocks than to information about the distribution itself. Thus, due to the fact that the ideal initial structure of blocks (and derivatives of it) is used, we see that the method gives a better approximation to the initial model of density distribution, with a larger α.

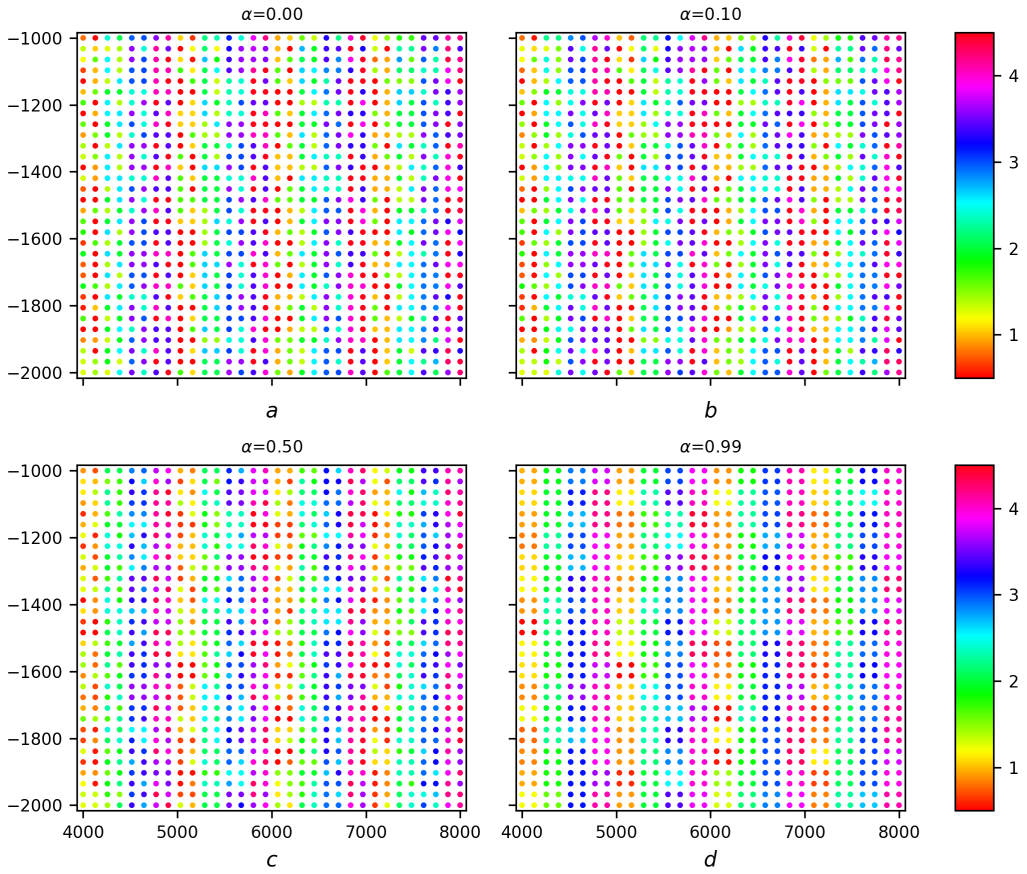

Figure 8. Finding a solution using the $F_{s\mu_2}$ functional on blocks 2×2: a – $\alpha = 0.0$, b – $\alpha = 0.1$, c – $\alpha = 0.5$, d – $\alpha = 0.99$.

Table 2. Quality criteria of obtained solutions for a priori distribution of densities μ_2

	Homogeneity	Closeness to ρ	Final criterion
$\alpha = 0.00$	—	15.39493	15.39493
$\alpha = 0.10$	12.37600	14.15752	13.97937
$\alpha = 0.50$	6.88721	9.70820	8.29771
$\alpha = 0.99$	0.14477	6.76424	0.21096

Example of finding a solution on the geological and geophysical model of the Norilsk Nickel deposit

Geological and geological-geophysical model of the deposit

The section of the liquation deposit of the Norilsk ore zone, known as of 2017 [*Kulikov*, 2017], was taken as the basis of the numerical model. The geological section of the Norilsk area in the first approximation is a subhorizontal-layered environment, represented (from bottom to top) by carbonate-terrigenous sediments of the Paleozoic, carbonized terrigenous sediments of the Tungussian series, stratified strata of basalts and tuffs of the main composition of the Permian – Lower Triassic (Figure 9) [*Kulikov*, 2017].

In spite of the fact that ore-bearing intrusions of Norilsk type are characterized by increased values of density, it is extremely difficult to identify in the observed gravity (dg) field anomalous effects from these objects. The reasons are: a relatively weak level of

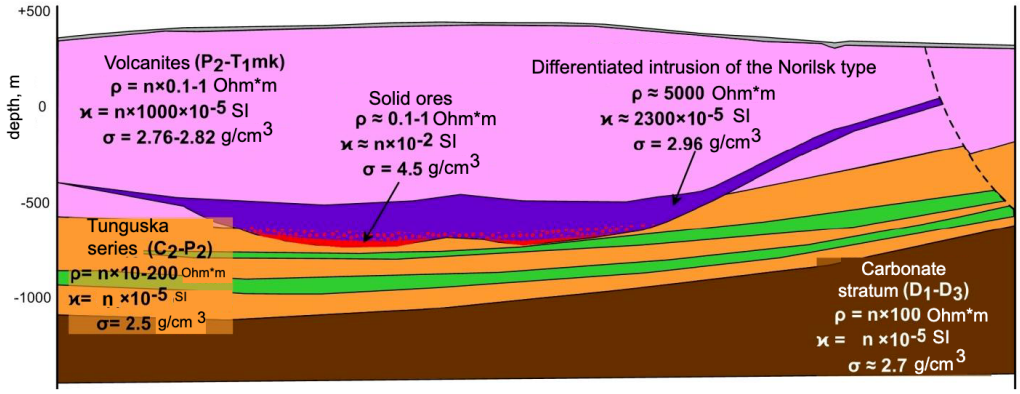

Figure 9. Generalized petrophysical model of the section that is typical for the Norilsk ore zone [*Kulikov*, 2017].

Table 3. Petrophysical characteristics of the Norilsk ore zone section [*Kulikov*, 2017]

Horizons		Density, g/cm^3
Quaternary (Q)		2.22
Mokulaevskaya Formation (T_1mk) Moronga Formation (T_1mr) Nadezhdinskaya Formation (T_1nd) Khakancha Formation (T_1hk + gd) Syverminskaya Formation (T_1sv) Ivakinsky Formation (P_1iv)	Vulcanites (Basalts)	2.72–2.82
Tunguska series ($C_2 - P_2$)		2.5
United ($D_2 - D_3$)	Carbonate Strata	2.78
Manturovskaya Formation (D_2mt)		2.76
Razvedochninskaya Formation (D_1rz)		2.67
Kureya Formation (D_1kr)		2.73
Zubovskaya Formation (D_1zb)		2.76
Intrusions of the Norilsk type		2.9–3.1
Ore-Free Intrusions		2.95-3
Solid Ores		4.5
Disseminated Ores		4

the useful signal; the presence of intense anomalies-interference due to physical inhomogeneities of the surrounding environment; specific distortions of anomalies associated with the mountainous terrain, etc [*Kulikov*, 2017].

Under favorable conditions, differentiated ore-bearing intrusions, at depths of up to 1200–1500 m, can be detected by means of gravity prospecting. Ore knots, which are a set of spatially convergent ore-bearing intrusions, can be detected by gravity survey at depths of up to 3000 m [*Kulikov*, 2017].

Based on the above data on the form of occurrence of layers, intrusions and their properties, a two-dimensional geological and geophysical model of the section typical for

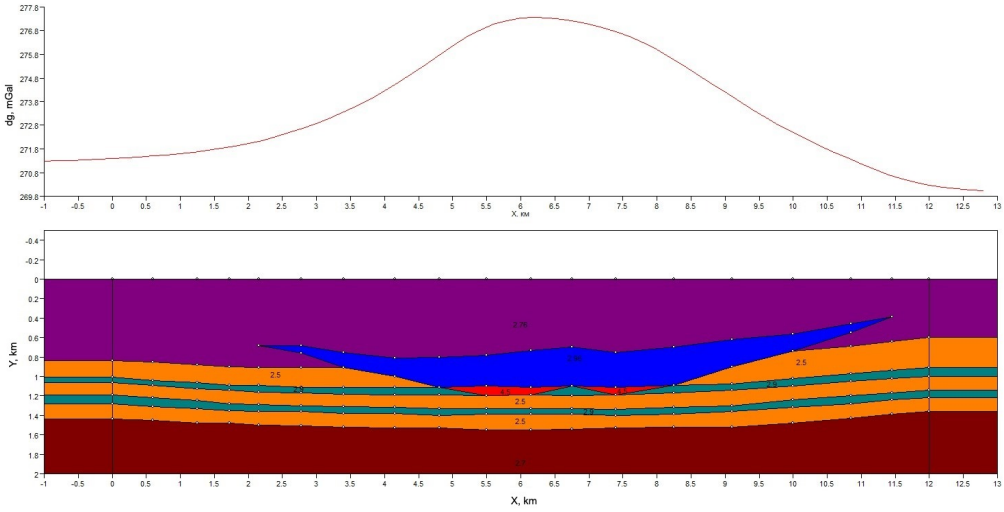

Figure 10. Geological and geophysical model created on the basis of data on the Norilsk ore zone.

the Norilsk ore zone was created. This model is shown in Figure 10, distance in km, density in g/cm^3.

Results of the search for solutions

To solve the direct gravity problem for the two-dimensional model, we used the complex variable function theory for a polygon with constant density [*Bulychev et al.*, 2010].

The system $Ax = b$ describes the gravitational effect of the dense environment. The system of linear equations can be written as follows, by analogy with the system (21):

$$[a_{ji}][x_i] = [b_j] \tag{22}$$

where x_i are the unknown densities, a_{ji} is the effect of $i - o$ block at observation point j, b_j is the value of the observed field at point j.

In order to apply the projection method, the two-dimensional model of the section (Figure 10) was split into blocks (Figure 11). The resulting model is called the "initial" model, and we assume that we know only the observed field from this model. During the study, we assume that only the useful signal is selected in the observed field and that there is no noise component in it. Also, to take advantage of the ability to account for the F_s functional, let us represent our existing model as a density grid, 50 by 60 cells horizontally and vertically, with dimensions of 240 m horizontally and 40 m vertically, assigning cells to the density of the original model and relating each cell to the block model of the Figure 11. The resulting model is shown in Figure 12.

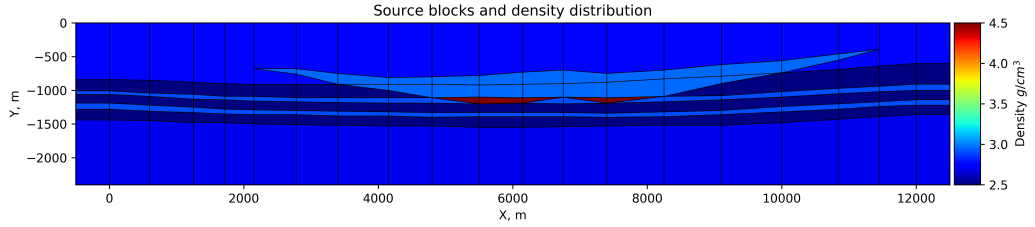

Figure 11. Initial geological and geophysical model split into blocks.

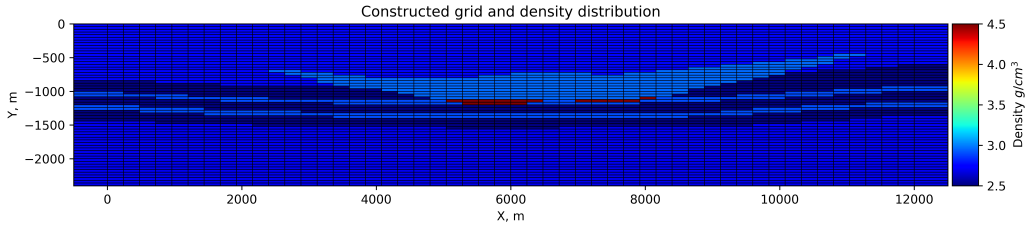

Figure 12. Initial geological and geophysical model represented in the form of a grid.

The method was tested on a geological geophysical example, taking into account a priori information about the density distribution and block structures consisted of cells.

First, we show the dependence of the result on α. The block structures for each example are constant, a noisy initial model of 0.3 g/cm^3 has been used as the density distribution, α is taken equal to 0.0, 0.1, 0.3, 0.5, 0.9, 1.0. The standard deviation of the obtained solution from the original density distribution is shown in the Table 4. We see that when α equals 1.0, when only the formalization of E_S is included in the solution, the deviation is the largest, and the best value of α is chosen by the interpreter when he tries to find a compromise between the two statements $E_\mu \wedge E_S$.

Table 4. The standard deviation of the resulting solution from the original density distribution for different α

α	$\|\|x - x^f\|\|$
0.0	7.46037
0.1	6.75904
0.3	5.37339
0.5	4.03042
0.9	1.88739
1.0	3102.58

We show the results of inverse problem solutions for different α under different initial conditions. The block structures for each example are constant, a noisy initial model was used as the density distribution, at 0.1, 0.3 and 0.5 g/cm^3, α is taken equal to 0.1, 0.5, 0.9, 0.9(9). The results of the search for solutions are shown in the figures below. It can be seen that the gravitational field from the resulting models when solving the inverse problem coincides with the original observable field. It is also seen that the resulting model visually approximates the original model as α increases. However, it is worth noting that at α equal to 0.9(9) we see a picture of highly inhomogeneous medium, since almost no a priori information about the initial density distribution is taken into account.

Appendix A presents the plots (Figures A1–A21) of the observed field for the original model, the model after partitioning into cells, noisy a priori information, and the result of the solution search are also presented.

Conclusion

The projection method with respect to the system $Ax = b$ consists in efficiently constructing the variety of its solutions $\Phi(A, b)$. In the present paper this is done using the Gramm-Schmidt orthogonalization.

Knowledge of $\Phi(A, b)$ allows us to take into account a priori expert information about the properties of the solution x^f and restrict its search to $\Phi(A, b)$. In this paper, this is done for three expert statements: E_μ, E_S and their conjunction $E_{\mu S} = E_\mu \wedge E_S$.

The judgement E_μ about the similarity of the solution x^f with the known vector μ is implemented on $\Phi(A,b)$ in two ways. It is shown by examples that each of them works better than the traditional way of accounting for μ based on Tikhonov regularization.

The E_S judgement of S-homogeneity of x^f by itself is of little use due to great ambiguity, but its coupling to $E_{\mu S}$ with the scheme E_μ gives good results: if the initial solution x^f is indeed S-uniform, then the result $x_{\mu S}$ of its search by the scheme $E_{\mu S}$ turns out to be closer to x^f than the result x_μ of the search by the scheme E_μ: $\left\|x_{\mu S} - x^f\right\| < \left\|x_\mu - x^f\right\|$ (based on the results for finding a solution for the ore problem based on the geological geophysical model of the Norilsk Nickel deposit).

In reality, information x^f is fuzzy: the expert knows more about some things and less about others. Therefore, the authors see a natural extension of research in constructing fuzzy variants of schemes, E_μ, E_S, $E_{\mu S}$.

Acknowledgments. This work was funded by the Russian Science Foundation (project No. 24-17-00346).

Appendix A

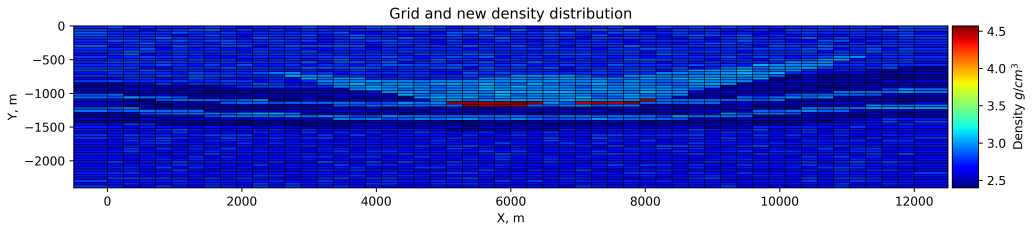

Figure A1. Noisy a priori model at 0.1 g/cm^3.

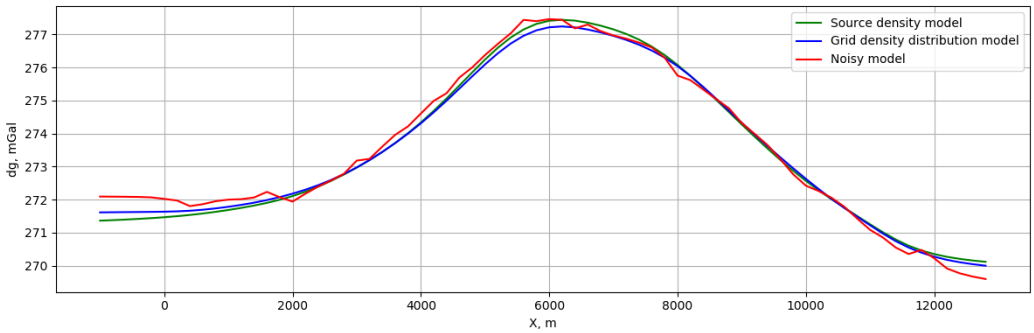

Figure A2. Comparison of observed field plots from the original cell-split model and the a priori model at 0.1 g/cm^3 noisiness.

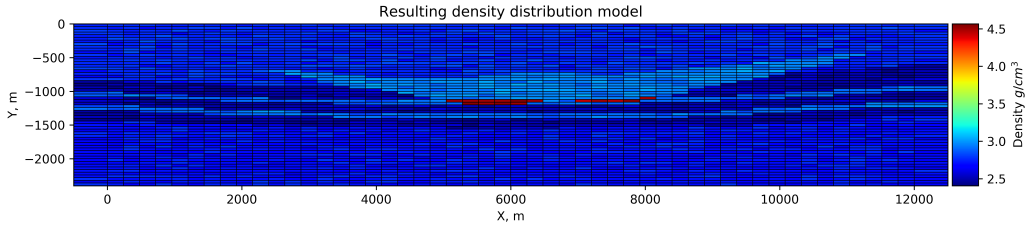

Figure A3. The result of searching for a solution using an a priori model with a noise of 0.1 g/cm^3 and α equal to 0.1.

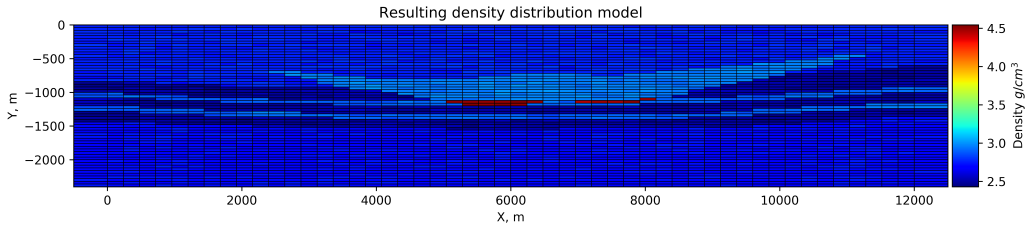

Figure A4. The result of searching for a solution using an a priori model with a noise of 0.1 g/cm^3 and α equal to 0.5.

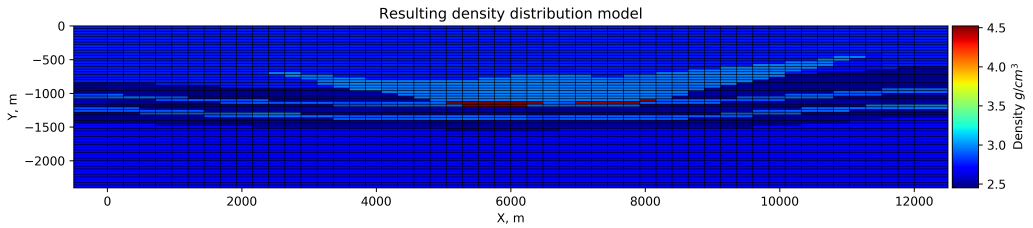

Figure A5. The result of searching for a solution using an a priori model with a noise of 0.1 g/cm^3 and α equal to 0.9.

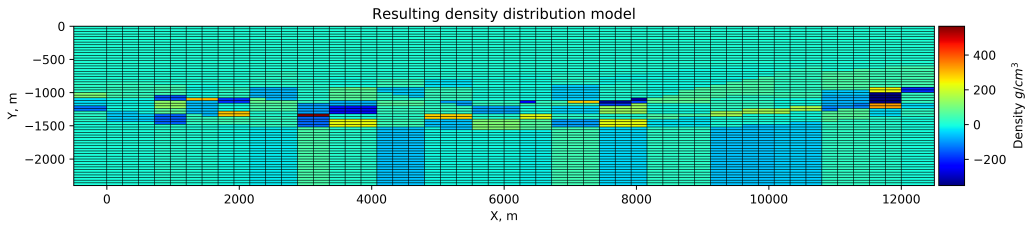

Figure A6. The result of searching for a solution using an a priori model with a noise of 0.1 g/cm^3 and α equal to 0.9(9).

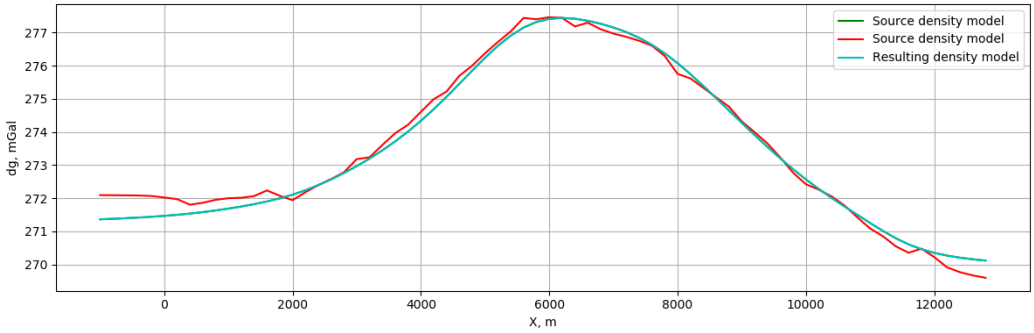

Figure A7. Comparison of observed field plots from the source model, the a priori model at 0.1 g/cm^3 noisiness and the resulting models.

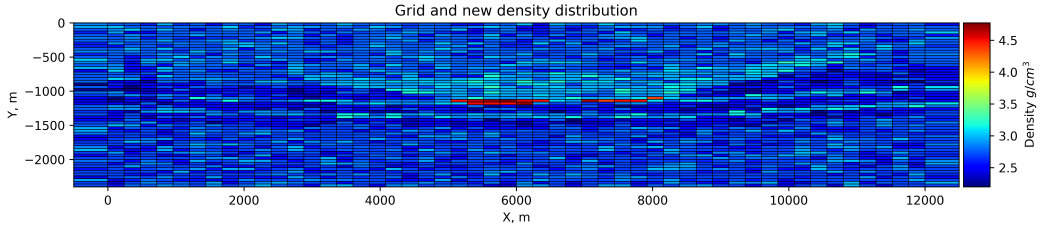

Figure A8. Noisy a priori model at 0.3 g/cm^3.

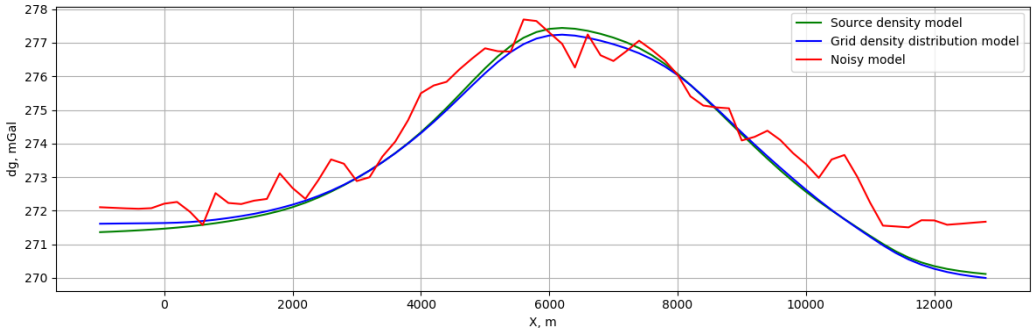

Figure A9. Comparison of observed field plots from the original cell-split model and the a priori model at 0.3 g/cm^3 noisiness.

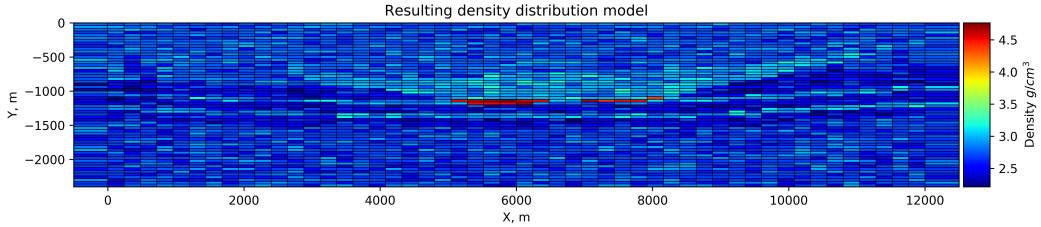

Figure A10. The result of searching for a solution using an a priori model with a noise of 0.3 g/cm^3 and α equal to 0.1.

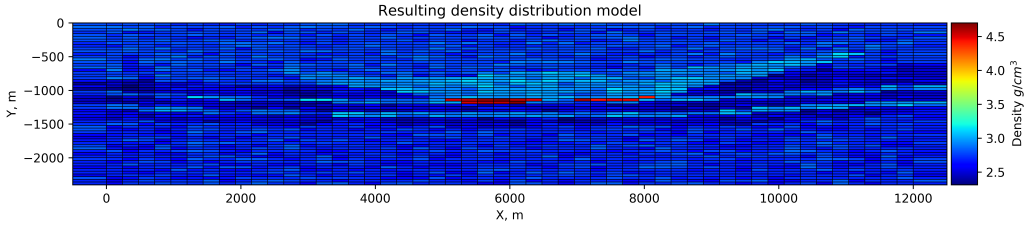

Figure A11. The result of searching for a solution using an a priori model with a noise of 0.3 g/cm^3 and α equal to 0.5.

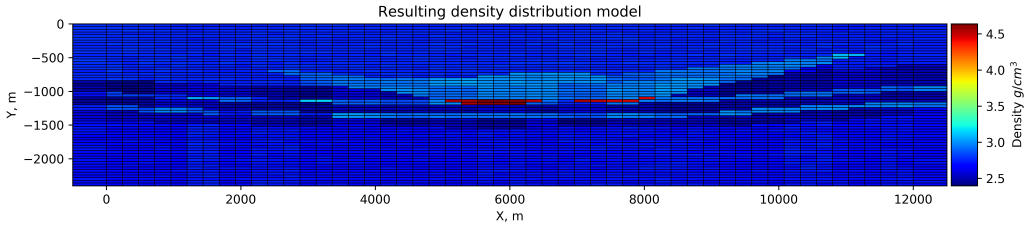

Figure A12. The result of searching for a solution using an a priori model with a noise of 0.3 g/cm^3 and α equal to 0.9.

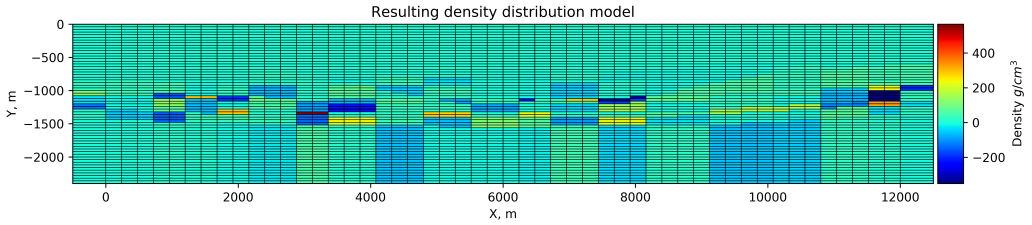

Figure A13. The result of searching for a solution using an a priori model with a noise of 0.3 g/cm^3 and α equal to 0.9(9).

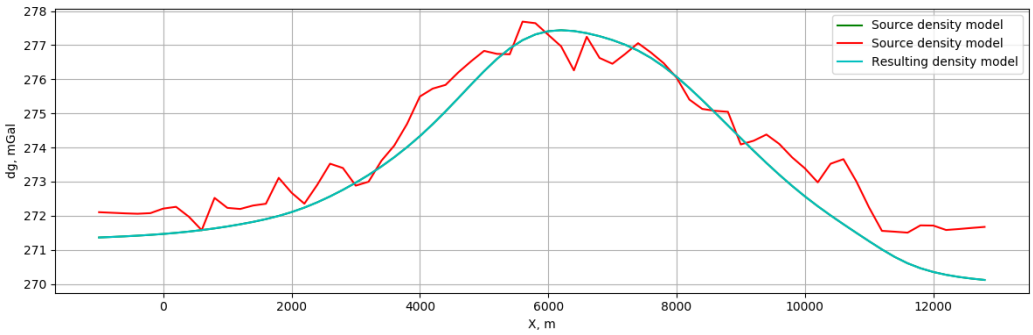

Figure A14. Comparison of observed field plots from the source model, the a priori model at 0.3 g/cm^3 noisiness and the resulting models.

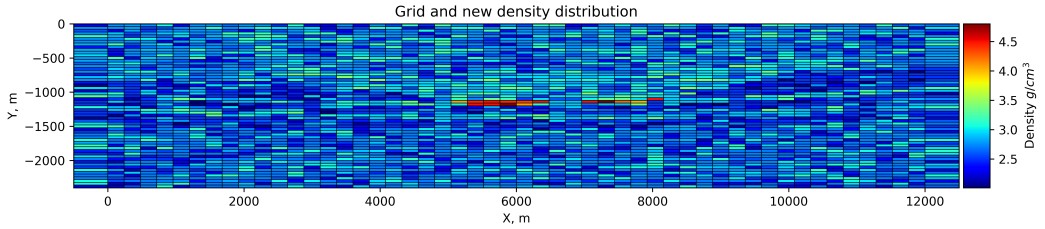

Figure A15. Noisy a priori model at 0.5 g/cm^3.

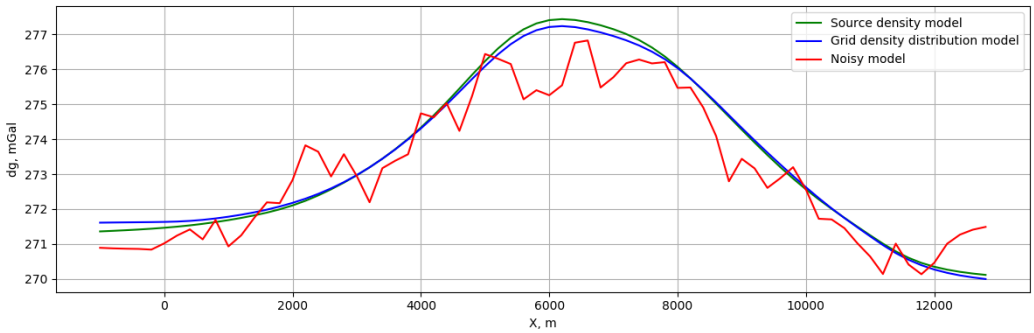

Figure A16. Comparison of observed field plots from the original cell-split model and the a priori model at 0.5 g/cm^3 noisiness.

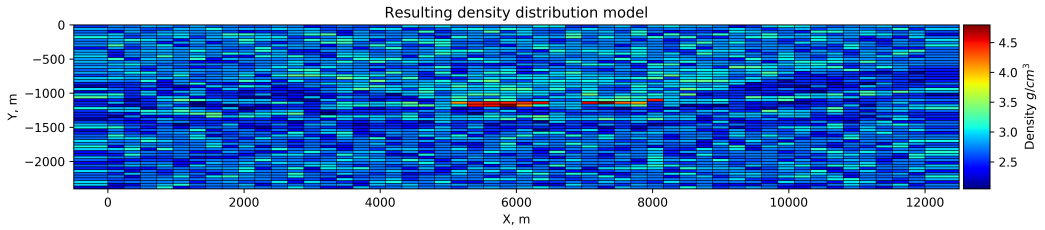

Figure A17. The result of searching for a solution using an a priori model with a noise of 0.5 g/cm^3 and α equal to 0.1.

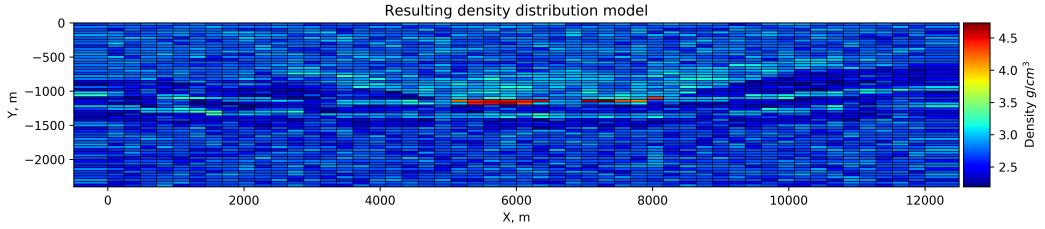

Figure A18. The result of searching for a solution using an a priori model with a noise of 0.5 g/cm^3 and α equal to 0.5.

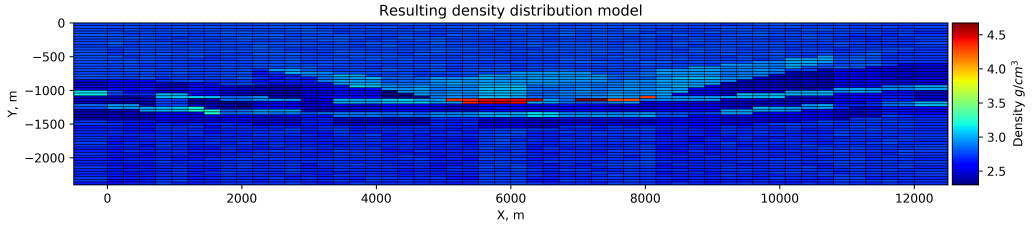

Figure A19. The result of searching for a solution using an a priori model with a noise of 0.5 g/cm^3 and α equal to 0.9.

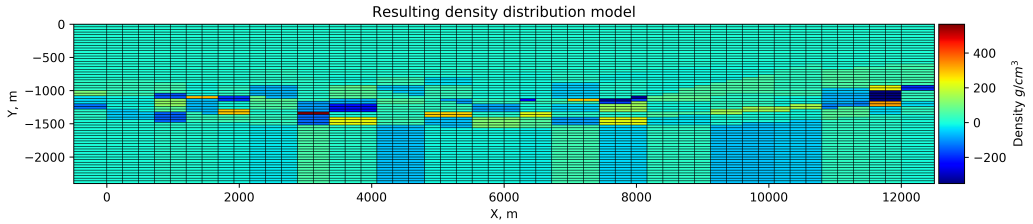

Figure A20. The result of searching for a solution using an a priori model with a noise of 0.5 g/cm^3 and α equal to 0.9(9).

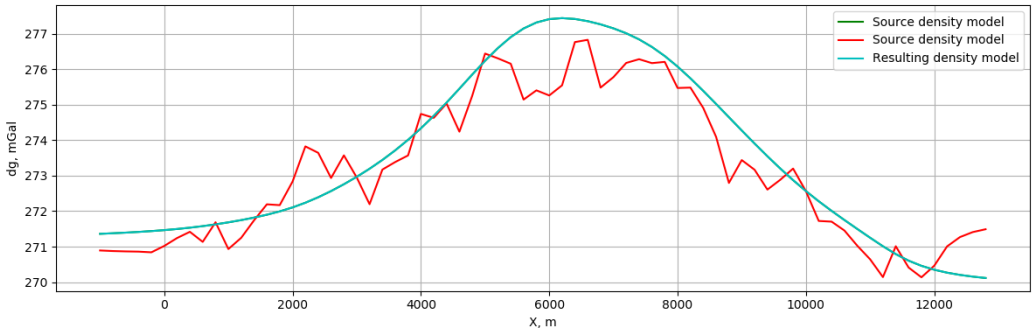

Figure A21. Comparison of observed field plots from the source model, the a priori model at 0.5 g/cm^3 noisiness and the resulting models.

References

Agayan, S. M., S. R. Bogoutdinov, A. A. Bulychev, A. A. Soloviev, and I. A. Firsov (2020), A Projection Method for Solving Systems of Linear Equations: Gravimetry Applications, *Doklady Earth Sciences*, *493*(1), 530–534, https://doi.org/10.1134/s1028334x20070053.

Bulychev, A. A., I. V. Lygin, and V. R. Melikhov (2010), *Numerical methods for solving direct problems of gravity and magnetic exploration (lecture notes)*, 164 pp., Geological Faculty of Moscow State University M. V. Lomonosov, Moscow (in Russian).

Kulikov, V. A. (2017), *Geophysics of solid field minerals*, 208 pp., PolyPRESS LLC, Moscow (in Russian).

Tikhonov, A. N., and V. Y. Arsenin (1979), *Methods for solving incorrect problems*, 283 pp., Nauka, Moscow (in Russian).

Turchin, V. F., and L. S. Turovtseva (1973), A method of statistical regularization with a posteriori estimation of the error in the original data, *Doklady Akademii Nauk SSSR*, *212*(3), 561–564 (in Russian).

Zelenyi, M., M. Poliakova, A. Nozik, and A. Khudyakov (2018), Application of Turchin's method of statistical regularization, *EPJ Web of Conferences*, *177*, 07,005, https://doi.org/10.1051/epjconf/201817707005.